THERMAL STABILITY AND THERMAL DECOMPOSITION KINETICS OF *GINKGO BILOBA* LEAVES WASTE RESIDUE

by

Changwei ZHANG[a,b], Chengzhang WANG[a,b*], Ran TAO[a,b], and Jianzhong YE[a,b]

[a] Institute of Chemical Industry of Forest Products, Chinese Academy of Forestry, Nanjing, China
[b] Key Laboratory of Biomass Energy and Material, Nanjing, Jiangsu, China

Original scientific paper
https://doi.org/10.2298/TSCI170117154Z

Non-isothermal thermogravimetric (TG) analysis was used to investigate the thermal stability and kinetics of three types of Ginkgo biloba leaves. These three types of Ginkgo biloba leaves included: Ginkgo biloba leaves before enzymolysis and ultrasound extraction (G1), Ginkgo biloba leaves after enzymolysis and ultrasound extraction (G2), and Ginkgo biloba leaves after soxhlet extraction (G3). Thermogravimetric/dynamic thermogravimetric, (dynamic TG) experiments indicated that the thermal stability of G2 and G3 were weaker than G1. Kissinger, Flynn-Wall-Ozawa, Friedman, and Coats-Redfern methods were firstly utilized to calculate the kinetic parameters and predicted decomposition mechanism of G1, G2, and G3. The thermal decomposition of G1, G2, and G3 were all corresponded to random nucleation and growth, following the Avrami-Erofeev equation, and activation energy of which were 191.4, 149.9, and 201.6 kJ/moL, respectively. In addition, the thermal decomposition G1, G2, and G3 were endothermic, irreversible and non-spontaneous.

Key words: *Ginkgo biloba leaves, thermal decomposition, kinetics, stability*

Introduction

Ginkgo biloba leaves (GBL) is a kind of traditional Chinese herbal medicine, which contains lots of active ingredients such as flavonoids, terpene lactones, and polyprenol [1-5]. In GBL, polyprenol is one of the most important active ingredients because of excellent biological activities [6-10]. As a result, the research on the extraction of polyprenol from GBL has always been a hotspot. Up to now, the primary method of extracting polyprenol from GBL is organic solvent extraction, but its extraction efficiency is low. For the sake of increasing extraction efficiency of polyprenol, a number of cell wall disruption technologies have been developed. Enzymolysis-based ultrasound extraction (EBUE) is a relatively new cell wall disruption method and is widely applied to the extraction of many active substance. Because it not only can increase the extraction efficiency but also be able to reduce the consumption of organic solvent [11, 12].

The EBUE of polyprenol from GBL was previously researched by Zhang *et al.* [13] and they found that the yield of polyprenol could reach 0.7954%, which represented an increase of 69.70% compared with the petroleum ether extraction. However, the GBL after extracting

* Corresponding author, e-mail: wangczlhs@sina.com

polyprenol were always thrown away as biomass waste. In fact, it could be reused in lots of field, especially in energy field. It is vital to study the thermal decomposition properties of these GBL waste residue. Because only knowing the thermal characteristics of these GBL waste residue, it can be thoroughly used at appropriate temperature. So far, many researches have been focused on the thermal decomposition and kinetics of biomass waste. Chen *et al.* [14] studied the thermal decomposition kinetics of microalgae residue, they discovered that biomass torrefaction at 300 °Cwith short duration is a more energy-saving route. Wang *et al.* [15] using Flynn-Wall-Ozawa method and Kissinger-Akahira-Sunose method to evaluate the pyrolysis kinetics of sawdust, and the range of activation energies for sawdust pyrolysis is between 101.53 and 114.83 kJ/ mol using Flynn-Wall-Ozawa method and is between 95.94 and 114.87 kJ/mol using Kissinger-Akahira-Sunose method. Viboon *et al.* [16] researched the thermal decomposition of *Jatropha curcas* L. waste, the results showed that pyrolysis of this residue may be applied for the production of value-added products as well as fuels after some upgrading processes.

Kinetics analysis have both practical application and theoretical application. The forecast of material lifetime and process rates is a main practical application of kinetics analysis. The description of the thermal decomposition process and determination of thermodynamic properties is theoretical application of kinetics analysis. But, there has no thermal decomposition kinetics analysis of GBL waste residue processed with EBUE been reported in literature. Therefore, TG technology was employed to analysis thermal stability, thermal decomposition kinetics, and thermodynamic properties of GBL waste residue. Meanwhile, Kissinger, Flynn-Wall-Ozawa, Friedman, and Coats-Redfern methods were adopted to determine activation energy, E, pre-exponential factor, A, reaction order and most probable mathematical reaction model of G1, G2, and G3, hoping to provide theoretical guidance for its thermal application in the future.

Materials and methods

Materials

The dried, smashed and screened G1, G2, and G3 (0.1~0.3 mm) were prepared at the Institute of Chemical Industry of Forest Products, Chinese Academy of Forestry, Jiangsu, China.

Experimental methods

The TG analysis were conducted under nitrogen atmosphere. A NETZSCH-TG 449C thermobalance was utilized over the temperature range of 308-923 K, the flow rate was 35 mL/ min, and the heating rates were 5, 10, 15, and 20 K/min, respectively. Kinetic researches of G1, G2, and G3 were performed using datas achieved from the TG analysis.

Thermal stability analysis

In order to evaluate the thermal stability of G1, G2, and G3, thermal decomposition index, I, was introduced. Moreover, the value of I has a negative correlation relationship with thermal stability. The expression of thermal decomposition index I is:

$$I = \frac{\left(\frac{d_\alpha}{d_t}\right)_{\max}}{T_{\max}\Delta T} \tag{1}$$

Thermal decomposition kinetics analysis

The analyses of thermal decomposition kinetics is often expressed by eq. (2) [17]:

$$\frac{d_\alpha}{d_t} = k(T) f(\alpha) \tag{2}$$

In eq. (2), $k(T)$ can be expressed by the eq. (3):

$$k(T) = A\mathrm{e}^{-E/\mathrm{R}T} \tag{3}$$

As $\beta = \mathrm{d}T/\mathrm{d}t$ under non-isothermal condition, the eq. (2) can also be expressed by eq. (4) [18]:

$$\frac{d_\alpha}{d_t} = \beta\frac{d_\alpha}{d_T} = A\mathrm{e}^{-E/\mathrm{R}T} f(\alpha) \tag{4}$$

Its integral form is:

$$g(\alpha) = \frac{A}{\beta}\int_0^T \mathrm{e}^{-E/\mathrm{R}T}\,\mathrm{d}T \tag{5}$$

where

$$g(\alpha) = \int_0^\alpha \frac{1}{f(\alpha)}\,\mathrm{d}\alpha \tag{6}$$

$\alpha = (m - m_\mathrm{o})/(m_\mathrm{f} - m_\mathrm{o})$ with m_o and m_f as the initial and final masses, respectively.

Friedman method

Friedman method is expressed by eq. (7) [19]:

$$\ln\left(\frac{d_\alpha}{d_t}\right) = \ln\left[Af(\alpha)\right] - \frac{E}{\mathrm{R}T} \tag{7}$$

By plotting $\ln(d_\alpha/d_t)$ *vs.* $1/T$, E value can be computed.

Kissinger method

Kissinger method is not involved in mechanism function, thus, the calculated result of E value is relatively correct. Kissinger method is expressed by eq. (8) [20-23]:

$$\ln\left(\frac{T_\mathrm{p}^2}{\beta}\right) = \ln\left(\frac{E}{\mathrm{R}}\right) - \ln A + \frac{E}{\mathrm{R}T_\mathrm{p}} \tag{8}$$

By plotting $\ln(\beta/T_\mathrm{p}^2)$ *vs.* $1/T_\mathrm{p}$, the values of E and A can be calculated.

Flynn-Wall-Ozawa method

This method does not need to be aware of reaction order, and it is an integral method [24].The Flynn-Wall-Ozawa method is represented by eq. (9):

$$\ln\beta = \ln\left(\frac{AE}{\mathrm{R}}\right) - \ln g(\alpha) + 5.3305 - 1.052\frac{E}{\mathrm{R}T} \tag{9}$$

By plotting lnβ *vs.* 1/T at certain conversion rates, the value of E can be calculated from the value of slope (−1.052E/R).

Coats-Redfern method

Coats-Redfern method is expressed by eq. (10) [25]:

$$\ln\left[\frac{g(\alpha)}{T^2}\right] = \ln\left[\frac{A\mathrm{R}}{\beta E}\left(1 - \frac{2\mathrm{R}T}{E}\right)\right] - \frac{E}{\mathrm{R}T} \tag{10}$$

Substituting $g(\alpha)$ of tab. 1 into eq. (10), and plotting ln[$g(\alpha)/T^2$] *vs.* 1/T, E values of different reaction mechanism functions can be calculated based on the slope (−E/R).

Supposing:

$$f(\alpha) = (1-\alpha)^n \tag{11}$$

$$g(\alpha) = \frac{1-(1-\alpha)^{1-n}}{1-n} \tag{12}$$

For the most of E values and ordinary reaction temperature T, $E/\mathrm{R}T >> 1$. Thus, ln[AR(1 – 2RT/E)/βE] = constant. By plotting ln[$g(\alpha)/T^2$] against 1/T, the E values of different mathematical reaction models can be achieved according to the value of slope (−E/R).

Determination of the most probable mathematical reaction model

On account of compensation effect exists in the activation energy and pre-exponential factor, leading to the kinetic parameters of same substance are different. It is obvious that the difference between selected mathematical reaction model form and actual kinetic process is primary cause. Thus, the selection of the most probable mathematical reaction model is crucial. For the objective of choosing the most probable mathematical reaction models of G1, G2, and G3, forty kinds of kinetic mathematical reaction models (see tab. 1) were substituted into Coats-Redfern equation to calculate the values of activation energy, severally. The E values obtained from Coats-Redfern method which are nearest to the range of E values gained from Kissinger, Friedman, and Flynn-Wall-Ozawa methods are the most probable mathematical reaction models of G1, G2, and G3, separately.

Table 1. The algebraic expressions of $g(\alpha)$ for forty kinds of mathematical reaction models

No.	$g(\alpha)$	No.	$g(\alpha)$	No.	$g(\alpha)$	No.	$g(\alpha)$
1	α^2	11	$[-\ln(1-\alpha)]^{1/3}$	21	$\ln[\alpha/(1-\alpha)]$	31	$1-(1-\alpha)^{1/2}$
2	$\alpha+(1-\alpha)\ln(1-\alpha)$	12	$[-\ln(1-\alpha)]^{2/5}$	22	$\alpha^{1/4}$	32	$1-(1-\alpha)^2$
3	$[1-(1-\alpha)^{1/2}]^{1/2}$	13	$[-\ln(1-\alpha)]^{1/2}$	23	$\alpha^{1/3}$	33	$1-(1-\alpha)^3$
4	$[1-(1-\alpha)^{1/2}]^2$	14	$[-\ln(1-\alpha)]^{2/3}$	24	$\alpha^{1/2}$	34	$1-(1-\alpha)^4$
5	$[1-(1-\alpha)^{1/3}]^{1/2}$	15	$[-\ln(1-\alpha)]^{3/4}$	25	α	35	$(1-\alpha)^{-1}$
6	$[1-(1-\alpha)^{1/3}]^2$	16	$-\ln(1-\alpha)$	26	$\alpha^{3/2}$	36	$(1-\alpha)^{-1}-1$
7	$1-2\alpha/3-(1-\alpha)^{2/3}$	17	$[-\ln(1-\alpha)]^{3/2}$	27	α^2	37	$(1-\alpha)^{-1/2}$
8	$[(1+\alpha)^{1/3}-1]^2$	18	$[-\ln(1-\alpha)]^2$	28	$1-(1-\alpha)^{1/4}$	38	$\ln\alpha$
9	$[(1-\alpha)^{-1/3}-1]^2$	19	$[-\ln(1-\alpha)]^3$	29	$1-(1-\alpha)^{1/3}$	39	$\ln\alpha^2$
10	$[-\ln(1-\alpha)]^{1/4}$	20	$[-\ln(1-\alpha)]^4$	30	$3[1-(1-\alpha)^{1/3}]$	40	$(1-\alpha)^{-2}$

Calculation of lnA

Equation (13) is utilized to estimate the value of ln$A$ [26]:

$$\ln A = aE + b \tag{13}$$

By fitting E and ln$A$ of most probable mathematical reaction model at different heating rate, the value of a and b can be got from the values of the slope and intercept. Thus, the value of ln$A$ can be calculated by substituting E into eq. (13).

Calculation of thermodynamic parameters

As the values of E and pre-exponential factor A were determined, thermodynamic parameters of thermal decomposition reaction can be acquired from eqs. (14)-(16) [27, 28]:

$$A\mathrm{e}^{(-E/\mathrm{R}T)} = \nu\mathrm{e}^{(-\Delta G/\mathrm{R}T)} = \frac{kT}{h}\mathrm{e}^{-(\Delta G/\mathrm{R}T)} \tag{14}$$

$$\Delta H = E - \mathrm{R}T \tag{15}$$

$$\Delta G = \Delta H - T\Delta S \tag{16}$$

Results and discussion

Thermal decomposition and thermal stability of G1, G2, and G3

The DTG-TG curves of G1, G2, and G3 were showed in fig. 1. As shown in fig. 1, it is concluded that DTG curve trends of G1, G2, and G3 are similar, and they all go through four stages, including dehydration stage, preheat decomposition stage, main thermal decomposition stage, and coke decomposition stage. In addition, TG and DTG curves shifted to higher temperature zone with the increase of heating rate, without changes in the kinetic curves, this is in accordance with the report of Esin *et al.* [29]. From the kinetics point of view, the thermal behavior suggests that the reaction rate is only function of the temperature and the thermal decomposition mechanism of the reaction is independent of the heating rate, at least under the experimental condition used in this study. The reason of appearing this phenomenon may be that the higher heating rate is, the time reached the same temperature is shorter and the extent of reaction for

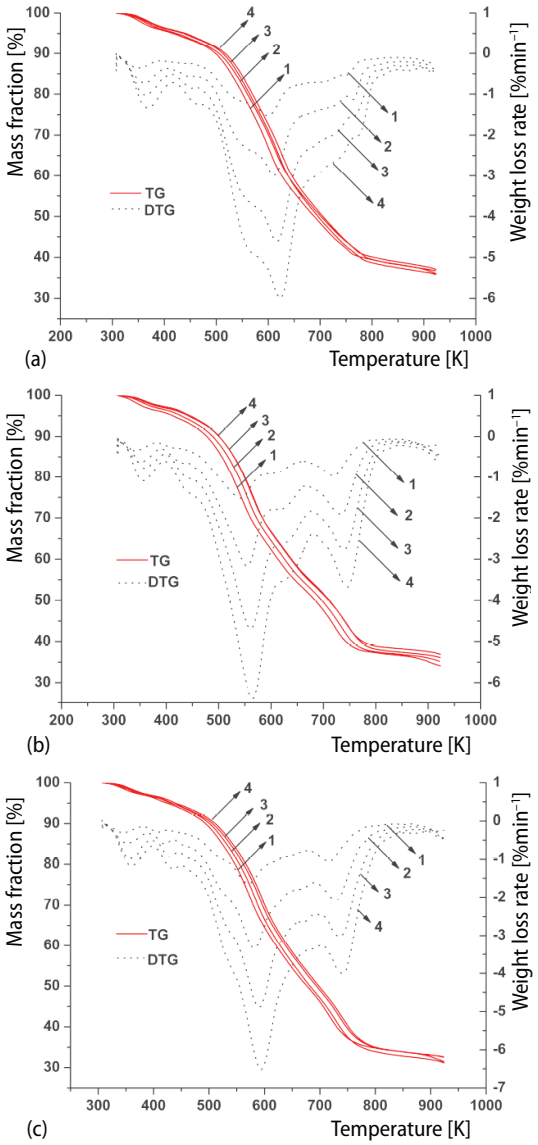

Figure 1. The TG-DTG curves of G1 (a), G2 (b), and G3 (c) at different heating rate; 1 – 5 K/min, 2 – 10 K/min, 3 – 15 K/min, 4 – 20 K/min

sample is lower. Meanwhile, the difference of heating rate caused the rate of heat transfer from internal to external was variational. In addition, heating rate directly influenced the temperature gradient of crucible sidewall and sample, leading to the phenomena of thermal hysteresis aggravated. The G1, G2, and G3 were turned into micro-molecular gases and macro-molecular condensable volatiles during main thermal decomposition stage, and the weight loss of this stage accounted for about 70% of total mass of decomposed sample. Therefore, subsequent kinetics analysis of G1, G2, and G3 mainly focused on this stage.

The thermal decomposition indexes of G1, G2, and G3 were showed in tab. 2. As shown in tab. 2, it was obvious that the I values of G2 and G3 were higher than G1, stating that G2 and G3 were easier to decompose than G1. This may be because that enzymolysis and ultrasound disrupted the structure of high stable ingredients such as cellulose in the cell wall of GBL, leading to the thermal stability of G2 and G3 reduced. In addition, it is clear that the thermal stability of G2 was lower than G3. The G2 was obtained by removing enzymatic hydrolysate, the enzymatic hydrolysate took away lots of water soluble ingredients from G2, in which some ingredients may be hard to decompose, resulting in G2 was easier to decompose. All in all, the thermal stability sequence of G1, G2, and G3 was that G2 < G3 < G1.

Table 2. Thermal decomposition indexes of G1, G2, and G3

Sample	T_1 [°C]	T_2 [°C]	T_{max} [°C]	$(d_\alpha/d_t)_{max}$ [%min^{-1}]	$I\cdot10^{-5}$
G1	200.7	465.7	336.7	2.92	3.273
G2	180.5	403.0	281.3	3.05	4.873
G3	195.3	420.3	308.2	2.97	4.283

Non-isothermal kinetic of G1, G2, and G3

The thermal decomposition kinetics of G1, G2, and G3 were investigated using Flynn-Wall_Ozawa (F-W-O), Friedman, Kissinger, and Coats-Redfern methods. The E values of G1, G2, and G3 calculated by the Kissinger method are 173.6, 140.5, and 168.4 kJ/moL, respectively. The values of ln$A$ are 35.36, 30.00, and 32.55, separately. In addition, the linear correlation coefficients, R^2, of G1, G2, and G3 are 0.9809, 0.9876, and 0.9876, singly. The kinetic parameters calculated by F-W-O and Friedman methods are given in tab. 3. As shown in tab. 3, the E values of G1, G2, and G3 calculated by F-W-O and Friedman methods increased with the rise of conversion. This may be because that the exist of hemicellulase, cellulose, and lignin caused the thermal decomposition of GBL become harder and harder with the reaction going on. In addition, the values of activation energy achieved from F-W-O method is slightly lower than Friedman method. All the linear correlation coefficients of G1, G2, and G3 were favorable, and the range of activation energy values for G1, G2, and G3 were 164.0-267.1, 110.8-219.7, and 146.2-221.4 kJ/moL, severally.

The kinetic parameters calculated with the Coats-Redfern method are listed in tab. 4. From tab. 4 it can be seen that the activation energy varied with the rise of heating rates. This is because the activation energy values tend to change with the heating rate for the same reaction model [30]. The range of E value for G1 calculated by aforementioned three kinds of methods was 164.0-267.1 kJ/mol. It was concluded that only E value calculated by 20 model was nearest to it. Therefore, it was inferred that 20 model could exactly describe the thermal decomposition process of G1. In a similar way, it was concluded that 19 and 20 model could exactly describe the thermal decomposition process of G2 and G3, respectively. Therefore, the decomposition mechanism of G1 corresponds to random nucleation and growth, following the Avrami-Erofeev equation with $n = 4$, integral form $g(\alpha) = [-\ln(1 - \alpha)]^4$; Decomposition mechanism of G2 and

Table 3. The related parameters of G1, G2, and G3 gained from F-W-O and Friedman method

Sample	F-W-O method						Friedman method					
	α	E	R^2	α	E	R^2	α	E	R^2	α	E	R^2
G1	0.05	164.0	0.9956	0.55	196.7	0.9996	0.05	172.6	0.9988	0.55	211.4	0.9998
	0.15	168.7	0.9982	0.65	204.5	0.9998	0.15	175.5	0.9986	0.65	219.0	0.9996
	0.25	172.3	0.9998	0.75	224.5	0.9870	0.25	179.5	0.9996	0.75	220.6	0.9998
	0.35	178.7	0.9998	0.85	242.5	0.9998	0.35	184.3	0.9998	0.85	262.0	0.9996
	0.45	183.5	0.9998	0.95	263.4	0.9998	0.45	195.2	0.9998	0.95	267.1	0.9998
G2	0.05	110.8	0.9998	0.55	165.0	0.9988	0.05	125.5	0.9998	0.55	169.6	0.9972
	0.15	124.4	0.9998	0.65	173.6	0.9988	0.15	133.8	0.9994	0.65	176.2	0.9996
	0.25	134.3	0.9998	0.75	185.2	0.9942	0.25	146.7	0.9996	0.75	184.1	0.9990
	0.35	145.8	0.9994	0.85	203.2	0.9996	0.35	159.3	0.9998	0.85	212.7	0.9902
	0.45	155.1	0.9994	0.95	217.1	0.9986	0.45	167.0	0.9987	0.95	219.7	0.9982
G3	0.05	146.2	0.9775	0.55	209.0	0.9934	0.05	161.5	0.9940	0.55	208.0	0.9894
	0.15	167.4	0.9930	0.65	219.2	0.9799	0.15	183.4	0.9928	0.65	209.2	0.9898
	0.25	187.7	0.9912	0.75	219.4	0.9898	0.25	201.9	0.9894	0.75	214.6	0.9892
	0.35	202.0	0.9912	0.85	221.3	0.9934	0.35	204.0	0.9894	0.85	219.6	0.9902
	0.45	204.4	0.9817	0.95	221.4	0.9833	0.45	207.7	0.9952	0.95	221.6	0.9829

Table 4. Kinetic parameters of G1, G2, and G3 obtained from Coats-Redferm method

	No.	β = 5 K/min			β = 10 K/min			β = 15 K/min			β = 20 K/min		
		E	ln$A$	$R2$	E	ln$A$	$R2$	E	ln$A$	$R2$	E	ln$A$	$R2$
G1	6	105.2	17.81	0.9992	109.2	19.02	0.9990	106.9	18.39	0.9994	110.2	19.21	0.9994
	16	41.75	5.804	0.9974	43.56	6.762	0.9980	43.09	6.822	0.9944	44.53	7.356	0.9940
	17	67.30	11.46	0.9980	70.09	12.54	0.9984	69.44	12.44	0.9956	71.63	13.09	0.9952
	18	92.86	16.95	0.9982	96.61	18.15	0.9986	95.79	17.91	0.9960	98.75	18.67	0.9956
	19	144.0	27.74	0.9984	150.0	29.19	0.9988	148.5	28.63	0.9964	153.0	29.63	0.9960
	20	195.1	38.39	0.9986	202.7	39.89	0.9988	201.2	39.63	0.9966	207.2	40.44	0.9962
G2	6	106.6	18.90	0.9952	112.5	20.57	0.9938	121.0	22.58	0.9789	118.4	22.10	0.9918
	14	24.57	2.034	0.9787	25.68	2.888	0.9845	26.62	3.444	0.9859	26.89	3.747	0.9859
	15	28.79	3.076	0.9807	30.07	3.949	0.9859	31.15	4.526	0.9870	31.45	4.828	0.9870
	16	41.46	6.092	0.9843	43.22	7.024	0.9884	44.75	7.661	0.9890	45.14	7.963	0.9892
	17	66.78	11.87	0.9868	69.53	12.92	0.9904	71.93	13.68	0.9906	72.52	13.98	0.9910
	18	92.10	17.50	0.9880	95.84	18.67	0.9912	99.12	19.55	0.9912	99.89	19.85	0.9918
	19	142.8	28.54	0.9890	148.5	29.95	0.9918	153.5	31.08	0.9918	154.6	31.38	0.9924
	20	193.4	39.45	0.9894	201.1	41.10	0.9922	207.9	42.48	0.9920	209.4	42.78	0.9928
G3	6	102.1	16.05	0.9918	104.5	16.85	0.9914	104.8	17.13	0.9928	104.8	17.11	0.9898
	17	63.67	9.898	0.9803	65.20	10.65	0.9799	66.31	11.18	0.9807	66.64	11.34	0.9734
	18	88.20	14.94	0.9823	90.30	15.71	0.9819	91.77	16.28	0.9825	92.28	16.40	0.9757
	19	137.3	24.81	0.9839	140.5	25.63	0.9837	142.7	26.26	0.9841	143.5	26.32	0.9779
	20	186.3	34.54	0.9847	190.7	35.41	0.9845	193.7	36.13	0.9849	194.8	36.10	0.9789
	6	102.1	16.05	0.9918	104.5	16.85	0.9914	104.8	17.13	0.9928	104.8	17.11	0.9898

G3 are the same with G1, and reaction order of G2 is $n = 3$, integral form $g(\alpha) = [-\ln(1 - \alpha)]^3$. Reaction order of G3 is $n = 4$, and integral form $g(\alpha) = [-\ln(1 - \alpha)]^4$.

Kinetic parameters and compensation effect of G1, G2, and G3 at different heating rate were showed in tab. 5 and fig. 2, respectively. Expressions of kinetic compensation effect

for G1, G2, and G3 were gained by fitting datas of tab. 5. Thereby, values of activation energy E and pre-exponential factor A for G1, G2, and G3 could be calculated. Activation energy E values of G1, G2, and G3 were obtained to be 201.6, 149.9, and 191.4 kJ/mol, respectively, and pre-exponential factor A values of G1, G2, and G3 were achieved to be $1.553\cdot10^{17}$, $1.352\cdot10^{13}$, and $2.752\cdot10^{15}$ min^{-1}, severally. Differential form, activation energy E value and pre-exponential factor A value of G1, G2, and G3 were separately substituted into the eq. (4), thus kinetic expressions of G1, G2, and G3 were displayed in eqs. (14)-(16), respectively. According to the actual E values of G1, G2, and G3, it is concluded that the thermal stability order of G1, G2, and G3 is that G2 < G3 < G1. This also proved the veracity of aforementioned thermal stability results of G1, G2, and G3.

Table 5. Kinetic parameters of G1, G2, and G3 gained from optimal model at different heating rate

	Heating rate [°Cmin^{-1}]	Fitted equation	Activation energy [kJ moL^{-1}]	ln$A$
G1	5	$y = -22.413x + 22.917$	186.3	34.54
	10	$y = -22.938x + 23.071$	190.7	35.41
	15	$y = -23.298x + 23.367$	193.7	36.13
	20	$y = -23.429x + 23.042$	194.8	36.10
G2	5	$y = -17.170x + 17.182$	142.8	28.54
	10	$y = -17.856x + 17.860$	148.5	29.95
	15	$y = -18.462x + 18.549$	153.5	31.08
	20	$y = -18.60x + 18.5550$	154.6	31.38
G3	5	$y = -23.465x + 26.719$	195.1	38.39
	10	$y = -24.381x + 27.683$	202.7	39.89
	15	$y = -24.198x + 26.424$	201.2	39.63
	20	$y = -24.919x + 27.323$	207.2	40.44

$$\frac{d_\alpha}{d_T} = \frac{1}{4}\cdot\frac{1.533\cdot10^{17}}{\beta}\exp\left(-\frac{201600}{8.314\cdot T}\right)(1-\alpha)[-\ln(1-\alpha)]^{-3} \tag{14}$$

$$\frac{d_\alpha}{d_T} = \frac{1}{3}\cdot\frac{1.352\cdot10^{13}}{\beta}\exp\left(-\frac{149900}{8.314\cdot T}\right)(1-\alpha)[-\ln(1-\alpha)]^{-2} \tag{15}$$

$$\frac{d_\alpha}{d_T} = \frac{1}{4}\cdot\frac{2.752\cdot10^{15}}{\beta}\exp\left(-\frac{191400}{8.314\cdot T}\right)(1-\alpha)[-\ln(1-\alpha)]^{-3} \tag{16}$$

Thermodynamic parameters of G1, G2, and G3

The values of E, A, and T of G1 were put into eq. (10)-(12), then the ΔH, ΔS, and ΔG values of G1 were obtained to be 196.7 kJ/mol, 13.71 kJ/(mol·K), 188.7 kJ/mol, respectively. In a similar way, ΔH, ΔS, and ΔG values of G2 were gained to be 145.3 kJ/mol, 31.29 J/(mol·K), 128.0 kJ/mol, respectively, and ΔH, ΔS, and ΔG values of G3 were achieved to be 186.3 kJ/mol, 36.35 kJ/(mol·K), 164.0 kJ/mol, respectively. All of values of ΔH, ΔS, and ΔG calculated from G1, G2, and G3 were greater than zero, stating that thermal decomposition of GBL and its waste residue are all endothermic, irreversible and non-spontaneous.

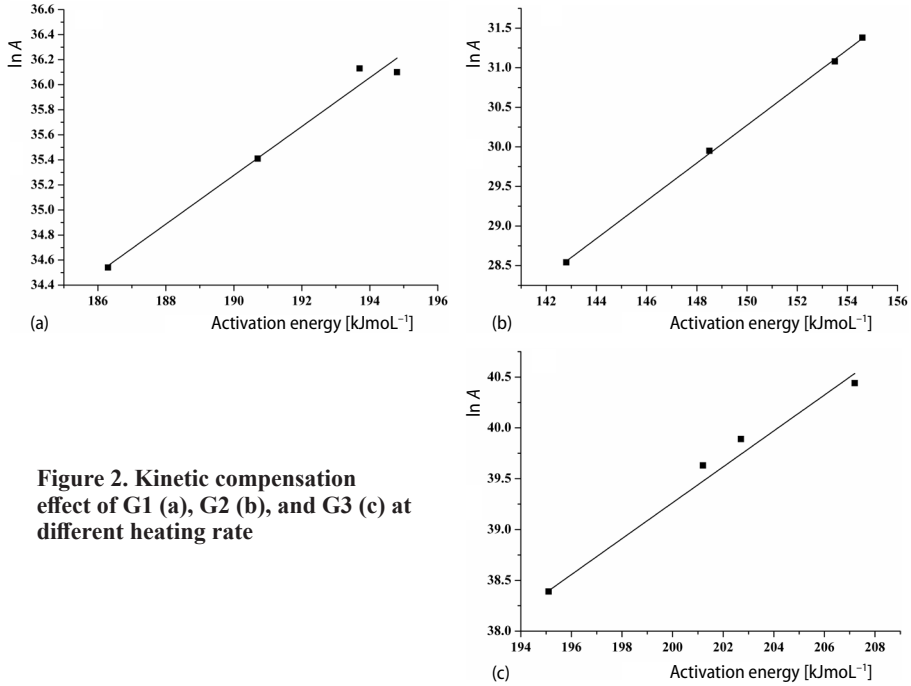

Figure 2. Kinetic compensation effect of G1 (a), G2 (b), and G3 (c) at different heating rate

Conclusion

The TG technology was successfully used to analysis thermal stability, thermal decomposition kinetics, and thermodynamic properties of G1, G2, and G3. The thermal stability order of G1, G2, and G3 is that G2 < G3 < G1. Non-isothermal decomposition mechanism of G1, G2, and G3 are all corresponded to random nucleation and growth, following the Avrami-Erofeev equation, and apparent activation energy values of G1, G2, and G3 are 201.6, 149.9, and 191.4 kJ/mol, respectively. In addition, the values of ΔH, ΔS, and ΔG of G1, G2, and G3 states that thermal decomposition of GBL and its waste residue are all exothermic, irreversible and non-spontaneous. These datas could provide theoretical references for the thermal application and reuse of G1, G2, and G3.

Acknowledgment

The support of this work by key laboratory of biomass energy and materials project of iangsu province (JSBEM-S-201708), innovative engineering project of research team building (LHSXKQ5) and national key research & development program of China (2016YFD0600805) are gratefully acknowledged.

Nomenclature

A – pre-exponential factor, [min^{-1}]
$(d_\alpha/d_t)_{max}$ – maximum weight loss rate, [%min^{-1}]
d_α/d_t – rate of conversion, [%]
E – apparent activation energy, [kJmol^{-1}]
ΔG – change values of Gibbs free energy, [kJmol^{-1}]
ΔH – change values of enthalpy, [kJmol^{-1}]
h – Planck constant, [6.625·10^{-34} Js^{-1}]
k – Boltzmann constant, [1.3807·10^{-23}]
R – gas constant, [8.314 Jmol^{-1}K^{-1}]
ΔS – change values of entropy, [kJmol^{-1}]
T – absolute temperature, [K]
T_{max} – temperature corresponding to maximum weight loss rate, [K]
T_p – absolute temperature of reaching maximum weight loss rate, [K]

ΔT – temperature of ending weight loss, [K]

Greek symbols

β – heating rate, [°Cmin^{-1}]
ν – Einstein vibration frequency, [Hz]

References

[1] Mahadevan, S., *et al*., Modulation of Cholesterol Metabolism by *Ginkgo Biloba* L. Nuts and Their Extract, *Food Research International*, *41* (2008), 1, pp. 89-95
[2] Singh, B., *et al*., Biology and Chemistry of *Ginkgo Biloba*, *Fitoterapia*, *79* (2008), 6, pp. 401-418
[3] Van Beek, T. A., Montoro, P., Chemical Analysis and Quality Control of *Ginkgo Biloba* Leaves, Extracts, and Phytopharmaceuticals, *Journal of Chromatography A*, *1216* (2009), 11, pp. 2002-2032
[4] Van Beek, T. A., Chemical Analysis of *Ginkgo Biloba* Leaves and Extracts, *Journal of Chromatography A*, *967* (2002), 1, pp. 21-55
[5] Wang, C. Z., *et al*., The Studies on the Chemistry, Purification and Pharmacology of Polyprenols from *Ginkgo Biloba* Leaves, *Natural Product Research and Development*, *13* (2000), pp. 43-45
[6] Defeudis, F. V., Drieu, K., "Stress-alleviating" and "Vigilance-enhancing" Actions of *Ginkgo Biloba* Extract (EGb 761), *Drug Development Research*, *62* (2004), 1, pp. 1-25
[7] Mahady, G. B., *Ginkgo Biloba* for the Prevention and Treatment of Cardiovascular Disease: A Review of the Literature, *Journal of Cardiovascular Nursing*, *16* (2002), 4, pp. 21-32
[8] Smith, J. V., Luo, Y., Studies on Molecular Mechanisms of *Ginkgo Biloba* Extract, *Applied Microbiology and Biotechnology*, *64* (2004), 4, pp. 465-472
[9] Yang, L., *et al*., Hepatoprotective Effects of Polyprenols from *Ginkgo Biloba* Leaves on CCl4-Induced Hepatotoxicity in Rats, *Fitoterapia*, *82* (2011), 6, pp. 834-840
[10] Tao, R., *et al*., Antibacterial/Antifungal Activity and Synergistic Interactions between Polyprenols and other Lipid Isolated from *Ginkgo Biloba* L. Leaves, *European Food Research and Technology*, *239* (2014), 4, pp. 587-594
[11] Farid, C., *et al*., Green Extraction of Natural Products Concept and Principles, *International of Journal Molecular Sciences*, *13* (2012), 7, pp. 8615-8627
[12] Rombaut, N., *et al*., Green Extraction Processes of Natural Products as Tools for Biorefinery, *Biofuels, Bioproducts and Biorefining*, *8* (2014), 4, pp. 530-544
[13] Zhang, C. W., *et al*., Enzymolysis-Based Ultrasound Extraction and Antioxidant Activities of Polyprenol Lipids from *Ginkgo Biloba* Leaves, *Process Biochemistry*, *51* (2016), 3, pp. 444-451
[14] Chen, W. H., *et al*., Thermal Decomposition Dynamics and Severity of Microalgae Residues in Torrefaction, *Bioresource Technology*, *169* (2014), 16, pp. 258-264
[15] Wang, J. X., *et al*., Error Evaluation on Pyrolysis Kinetics of Sawdust Using Iso-Conversional Methods, *Journal of Thermal Analysis and Calorimetry*, *124* (2016), 3, pp. 1-6
[16] Viboon, S., *et al*., Thermal Decomposition Study on *Jatropha Curcas* L. Waste Using TGA and Fixed Bed Reactor, *Journal of Analytical and Applied Pyrolysis*, *85* (2009), 1, pp. 155-162
[17] Li, X. Y., *et al*., Thermal Decomposition Kinetics of Nickel (II) and Cobalt(II) Azo Barbituric Acid Complexes, *Thermochimica Acta*, *493* (2009), 1, pp. 85-89
[18] Huang, M. X., *et al*., Thermal Decomposition Kinetics of Glycine in Nitrogen Atmosphere, *Thermochimica Acta*, *552* (2013), Jan., pp. 60-64
[19] Yao, F., *et al*., Thermal Decomposition Kinetics of Natural Fibers: Activation Energy with Dynamic Thermogravimetric Analysis, *Polymer Degradation and Stability*, *93* (2008), 1, pp. 90-98
[20] Rotaru, A., *et al*., Non-isothermal Kinetics of 2-Allyl-4-((4-(4-Methylbenzyloxy)Phenyl) Diazenyl) Phenol in Air Flow, *Journal of Thermal Analysis and Calorimetry*, *97* (2009), 2, pp. 485-491
[21] Rotaru, A., *et al*., Non-Isothermal Study of Three Liquid Crystals in Dynamic Air Atmosphere, *Journal of Thermal Analysis and Calorimetry*, *92* (2008), 1, pp. 233-238
[22] Kissinger, H. E., Variation of Peak Temperature with Heating Rate in Different Rate in Differential Thermal Analysis, *Journal of Research of the National Bureau Standards*, *57* (1956), 4, pp. 217-221
[23] Kissinger, H. E., Reaction Kinetic in Differential Thermal Analysis, *Analytical Chemistry*, *29* (1957), 11, pp. 1702-1706
[24] Ozawa, T., A New Method of Analyzing Thermogravimetric Data, *Bulletin of the Chemical Society of Japan*, *38* (1965), 11, pp. 1881-1886
[25] Xu, G., *et al*., Kinetic Study of Decomposition of Wheat Distiller Grains and Steam Gasification of the Corresponding Pyrolysis Char, *Journal of Thermal Analysis and Calorimetry*, *108* (2012), 1, pp. 109-117

[26] Chen, Z. P., *et al*., Application of Isoconversional Calculation Procedure to Non-isothermal Kinetic Study: III. Thermal Decomposition of Ammonium Cobalt Phosphate Hydrate, *Thermochimica Acta*, *543* (2012), 17, pp. 205-210
[27] Ma, H. X., et al., Synthesis, Molecular Structure, Non-Isothermal Decomposition Kinetics and Adiabatic Time to Explosion of 3,3-Dinitroazetidinium 3,5-Dinitrosalicylate, *Journal of Thermal Analysis and Calorimetry*, *95* (2009), 2, pp. 437-444
[28] Boonchom, B., Kinetics of Thermal Transformation of $Mg_3(PO_4)2.8H_2O$ to $Mg_3(PO_4)_2$, *Journal of Thermal Analysis and Calorimetry*, *31* (2010), 2, pp. 416-429
[29] Esin, A. V., *et al.*., Pyrolysis Kinetics and Thermal Decomposition Behavior of Polycarbonate-a TGA-FTIR Study, *Thermal Science*, *18* (2014), 3, pp. 833-842
[30] Vyazovkin, S., *et al*., ICTAC Kinetics Committee Recommendations for Performing Kinetic Computations on Thermal Analysis Data, *Thermochimica Acta*, *520* (2011), 1-2, pp. 1-19

Paper submitted: January 17, 2017
Paper revised: May 20, 2017
Paper accepted: June 14, 2017